# Pipeline Corrosion Monitoring by Fiber Optic Distributed Strain and Temperature Sensors (DSTS)


**Lufan Zou and Omur Sezerman**

***OZ Optics Limited***

**219 Westbrook Road, Ottawa, Ontario, Canada K0A 1L0**

**www.ozoptics.com**

**Winston Revie**

***CANMET Materials Technology Laboratory, Natural Resources Canada***

**Ottawa, ON, Canada**


# Fiber Optic Sensors

- Advantage of fiber optic sensors
  - Electrically insulating materials (no electric cables are required) — high voltage environments
  - Chemically passive, not subject e.g. to corrosion
  - Immune to electromagnetic interference (EMI)
  - Wide operation temperature range
- Fiber Bragg Grating Sensor
  - Strain resolution and accuracy: < 1 $\mu\varepsilon$
  - Non-distinguishable between strain and temperature
  - Point sensor
- Distributed Fiber Optic Sensors
  - Raman scattering based — only temperature
  - Brillouin scattering based — both temperature and strain

# Working Principle — BOTDA

## (Brillouin Optical Time Domain Analyzer)

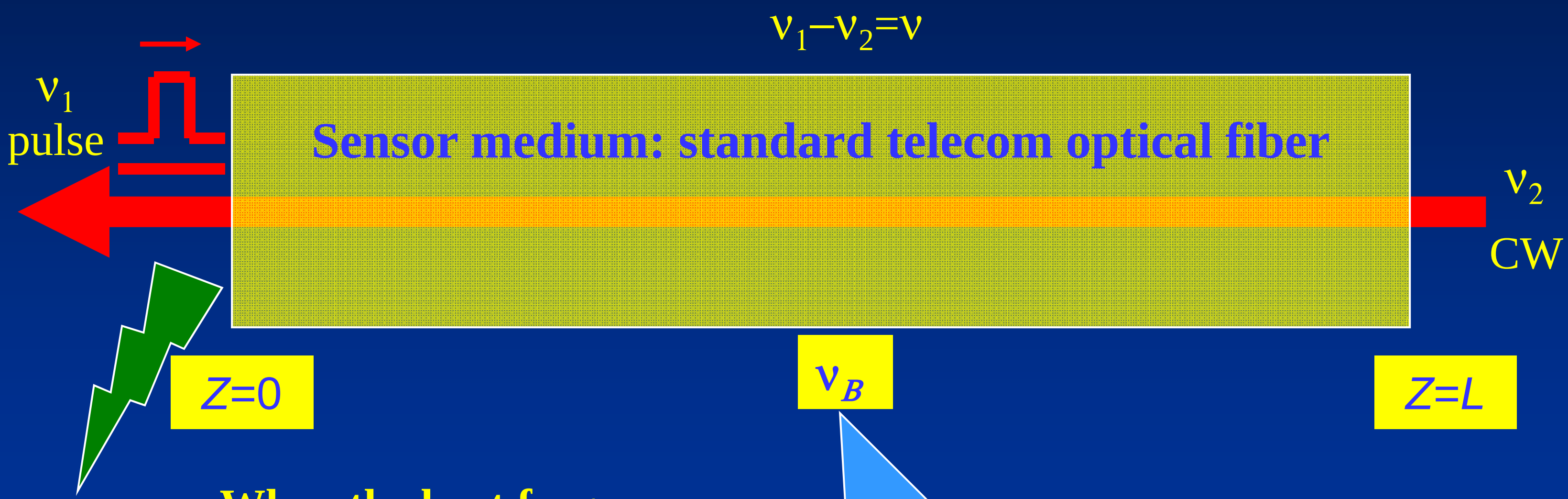


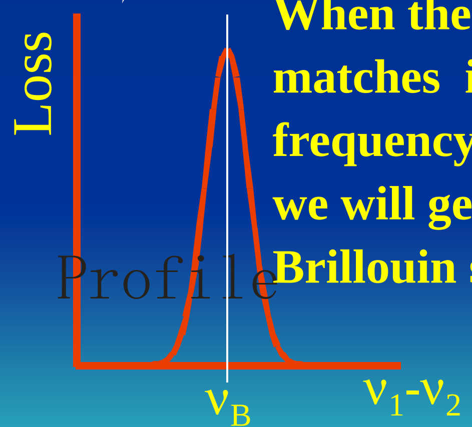


**Brillouin Spectrum**

**When the beat frequency $\nu$ matches intrinsic Brillouin frequency of the fiber $\nu_B$, we will get maximum of Brillouin spectrum.**

$\nu_B$ changes linearly with the strain and temperature exerted.

$$\nu_B = \nu_{B0} + C_T\left(T - T_0\right) + C_\varepsilon\left(\varepsilon - \varepsilon_0\right)$$

# Working Principle — BOTDA (cont'd)

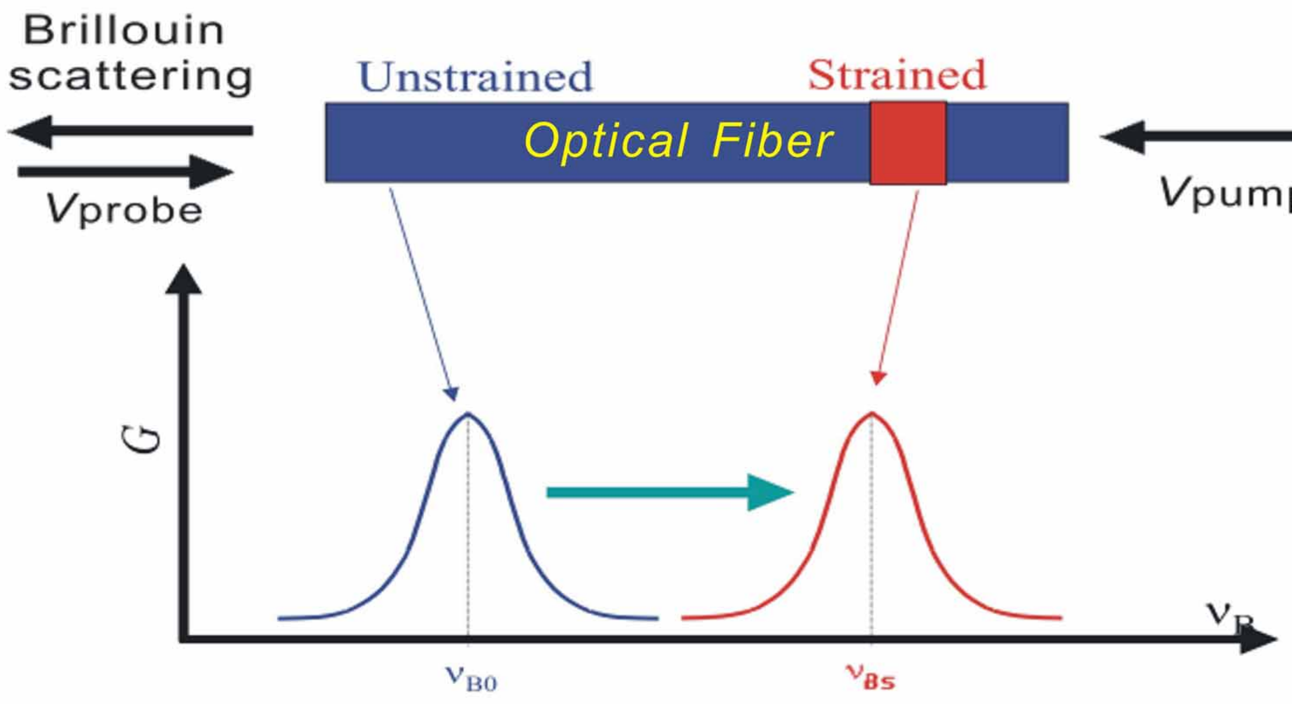


$$\nu_B = \nu_{B0} + C_T (T - T_0) + C_\varepsilon (\varepsilon - \varepsilon_0)$$

# Working Principle — Coherent interaction of pulse and pump lights

## Numerical model of P/P-based Brillouin Fiber Sensor

$$\left(\frac{\partial}{\partial z} - \frac{1}{v_g}\frac{\partial}{\partial t}\right)E_p = ig_1 Q E_s + \frac{1}{2}\alpha E_p$$

$$\left(\frac{\partial}{\partial z} + \frac{1}{v_g}\frac{\partial}{\partial t}\right)E_s = -ig_1 Q^* E_p - \frac{1}{2}\alpha E_s$$

$$\left(\frac{\partial}{\partial t} + \Gamma\right)\overline{Q} = -ig_2 E_p E_s^*$$

Three coupled differential equations:

* Two Maxwell's equations describing the propagation of the Stokes and pump laser beams

* A simplified Navier-Stokes equation describing the density wave

$\alpha$ = fiber absorption
$E_p$ = pump field
$E_s$ = Stokes field
$Q$ = acoustic field
$v_g = c/n$
$\Gamma = \Gamma_1 + i\Gamma_2$
$\Gamma_1 = 1/2\tau$
damping rate
$\Gamma_2 = \omega - \omega_B$
detuning frequency
$g_1$, $g_2$: coupling constants
$g_B = 2g_1g_2/\Gamma_1$
Brillouin gain

# Working Principle — Coherent interaction of pulse and pump lights (cont'd)

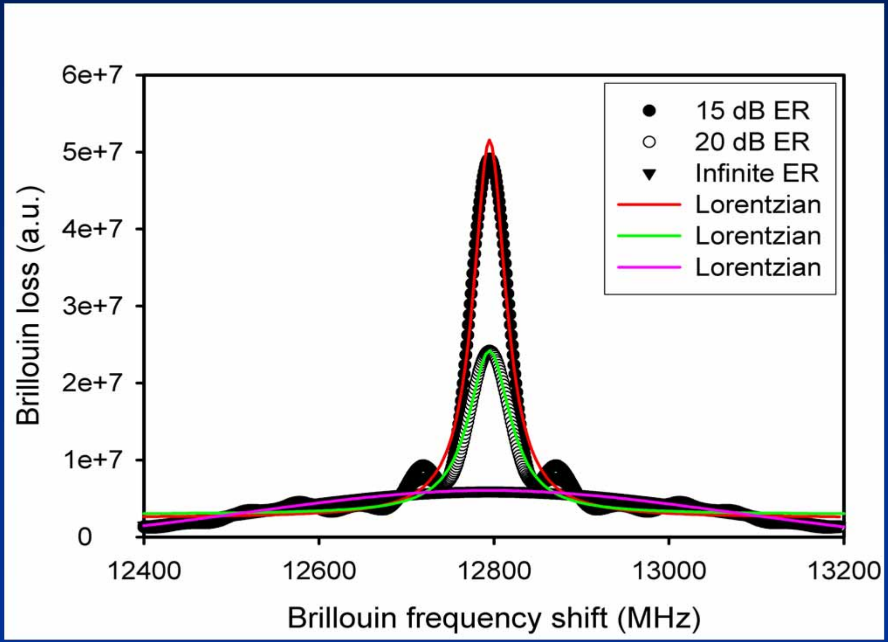


Numerical simulations
Pulse: 1.5 ns
Linewidth: 46, 58, and 952 MHz
for ER=15 dB, 20 dB, and infinite

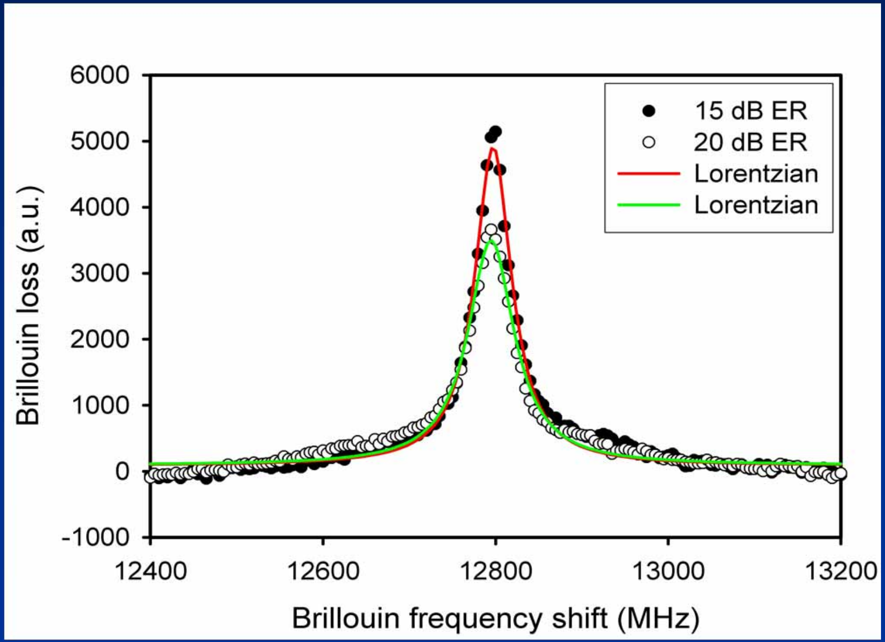


Experimental results
Pulse: 1.5 ns
Linewidth: 46 and 56 MHz
for ER=15 dB and 20 dB

# Applications


Oil and Gas Pipeline Monitoring


Dam Monitoring


Oil and Gas Well Monitoring


Bridge and Building Monitoring


Power Line Monitoring


Border Security Monitoring

Crack Detection

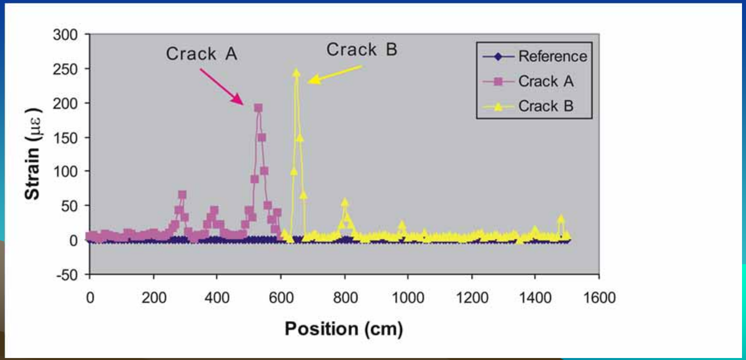

# Optical fiber layouts & sizes of depleted regions

**Parameters of cutouts (defects)**

| Cutout | Location (o'clock) | Reduced thickness (%) | Width (cm) | Length (cm) |
|---|---|---|---|---|
| *A* | 5-7 | 60 | 5.3 | 61 |
| *C* | 7 | 50 | 1.3 | 10 |
| *D* | 5 | 60 | 1.3 | 10 |


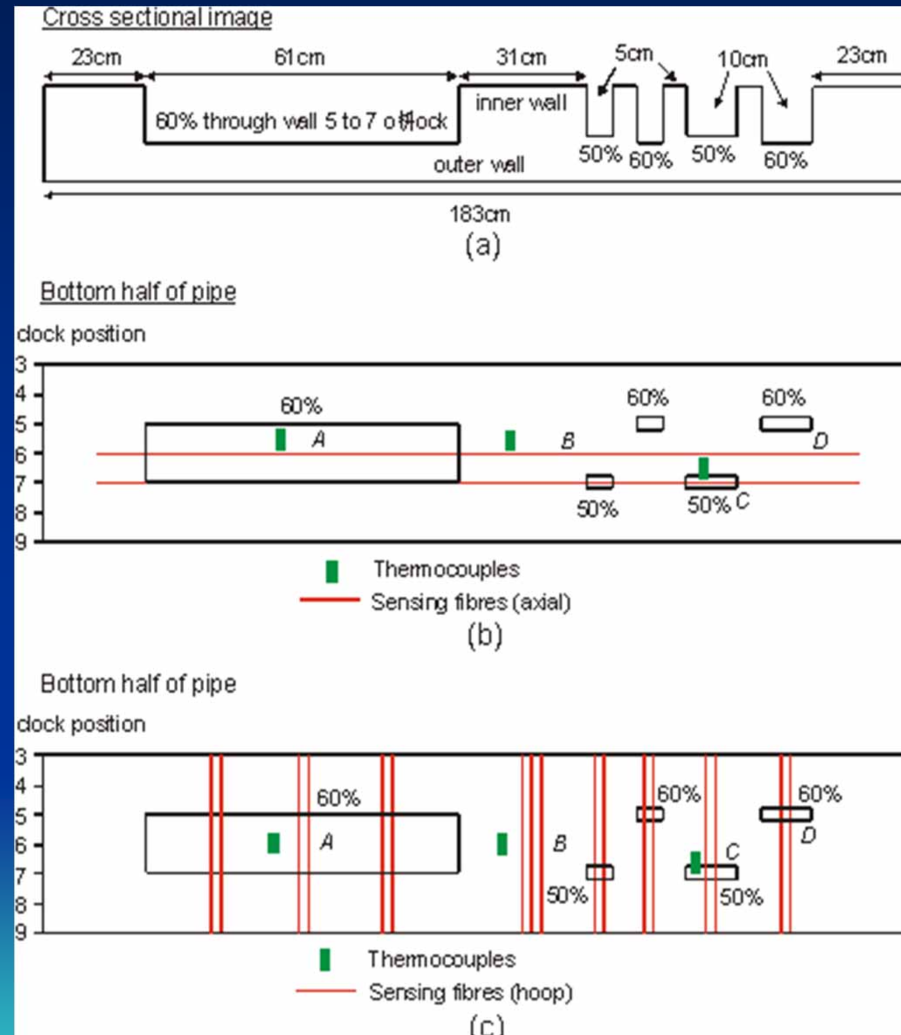

# Spectrum Shape

- The spectrum in the perfect region exhibits higher intensity
- Fiber experiences higher bending loss in defective region
- Coherent interaction of probe and pump lights produces complex spectrum
- These differences can be used to identify defective regions

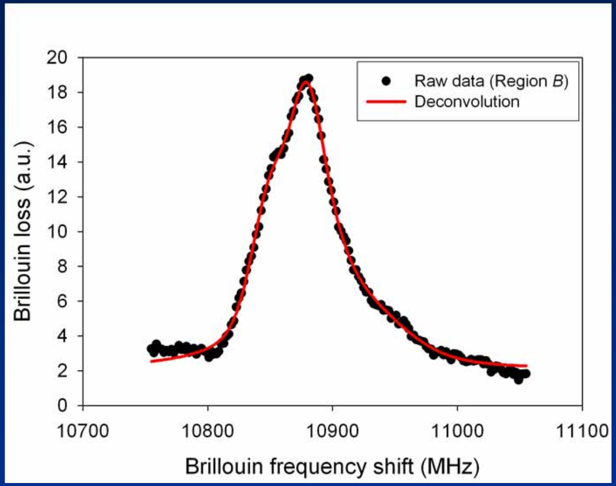


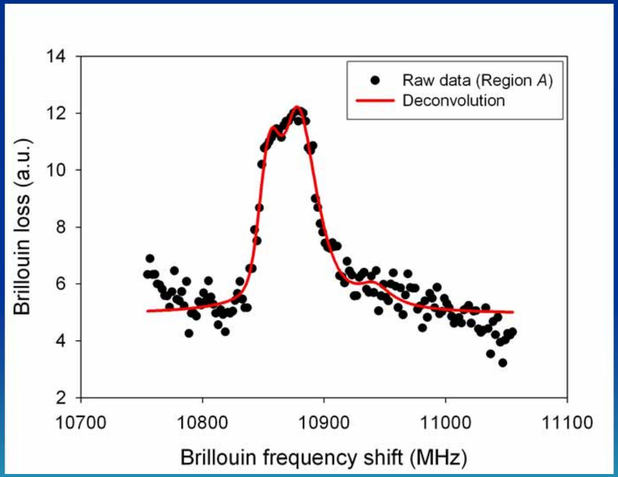

# Axial strain distribution

— along the pipe under 200 psi internal pressure

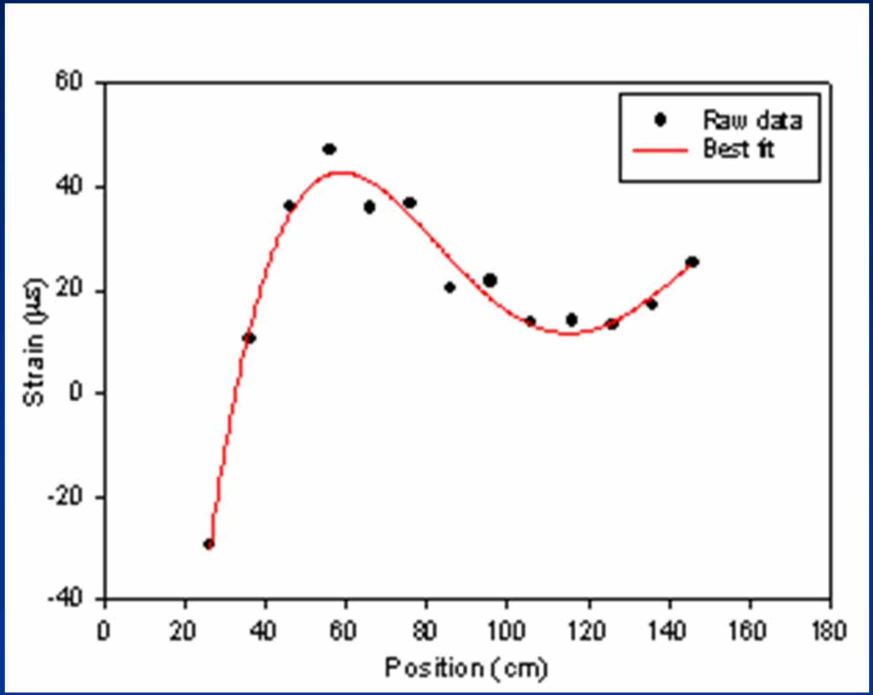


- Maximum strain (46 με) occurs in the middle of defect *A*.
- Minimum strain (14 με) happens in the middle of unperturbed region *B*.
- The support points, end-caps, asymmetric defect distribution affect axial strain distribution in both end of pipe.

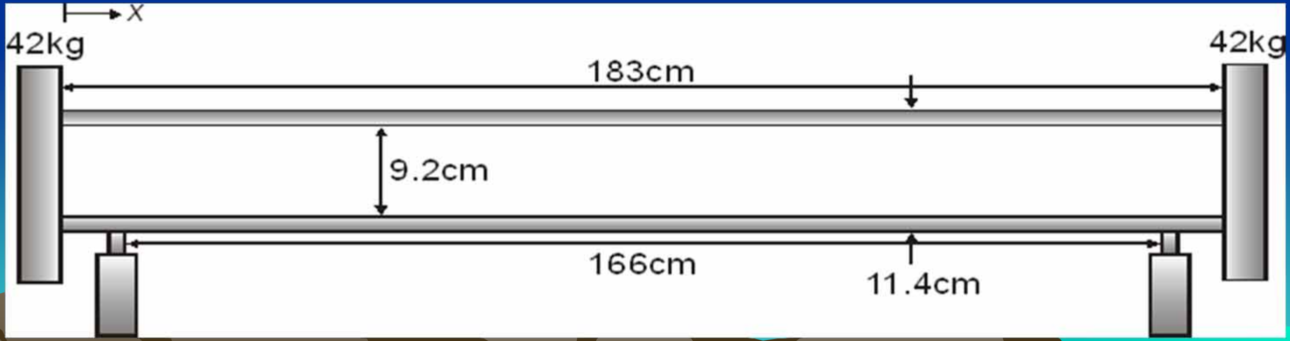

# Axial strain-pressure slopes

## — along the pipe

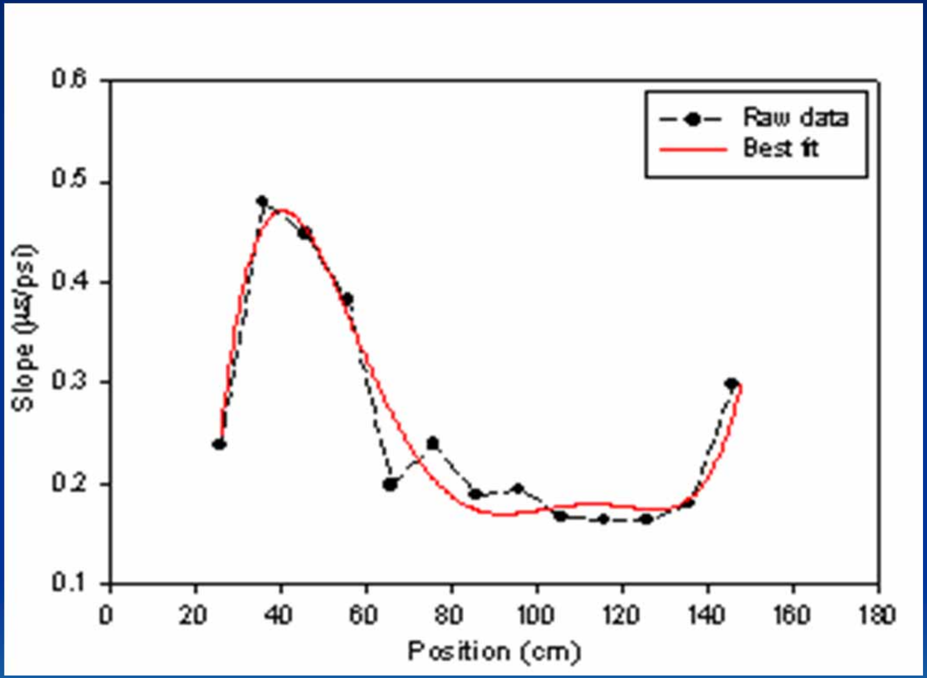


- Maximum 0.48 με/psi near the middle decreases toward the edges of defect *A*.
- Slope remains constant at 0.16 με/psi near the middle of unperturbed region *B*.
- Local stress concentration and overlapping 13 cm pulse lead to ripple from 70 to 100 cm.

# Comparison of axial strain

## — Defects *A* (60%) & *C* (50%) & region *B* (0%)

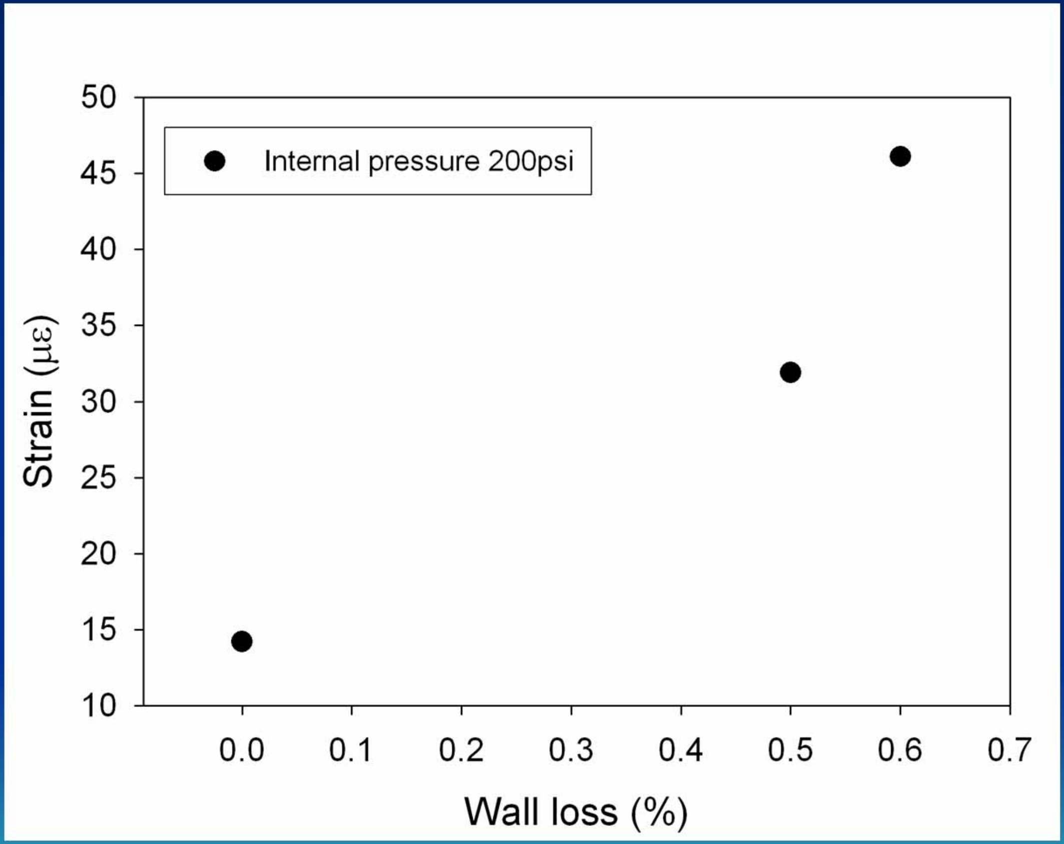

# Hoop strain distribution

Hoop strain distributions around one pipe circumference encompassing defective region *A* (*60% depleted wall, 5.3 cm wide and 61 cm long*). Two maximal strains, corresponding to one complete loop, are observed.

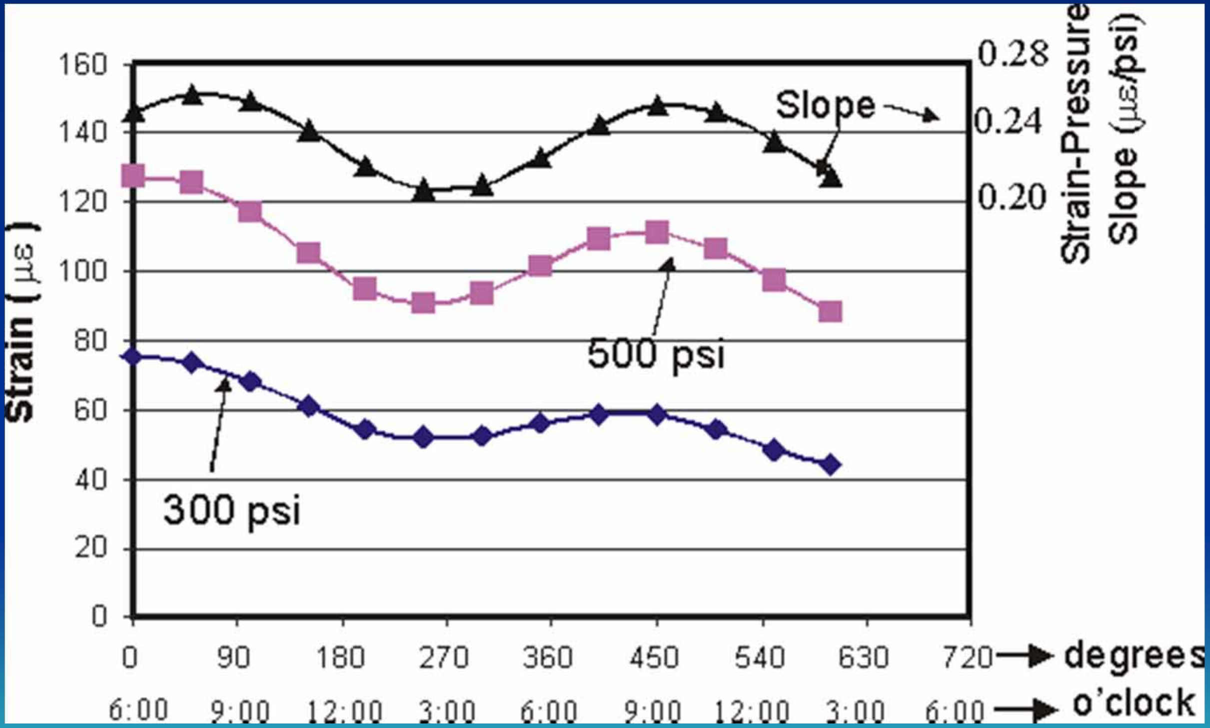


# Comparison of hoop strain

## — around defects *C* (50%) *& D* (60%)

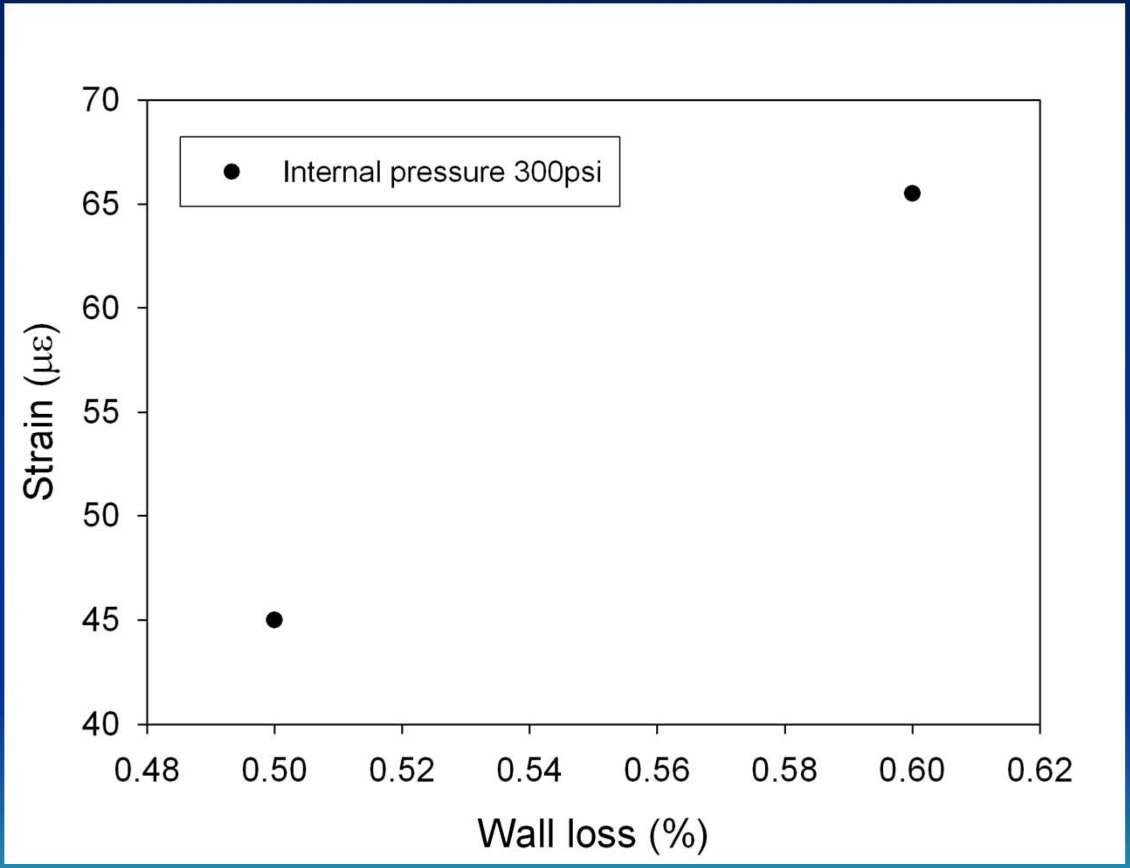

# Pipeline erosion monitoring by DSTS

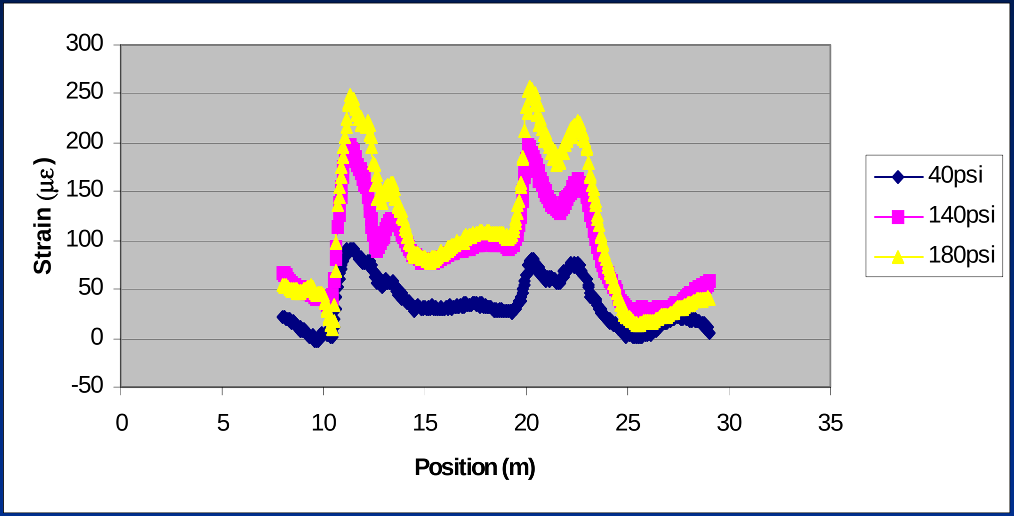


$$\varepsilon \propto \frac{p}{H}$$

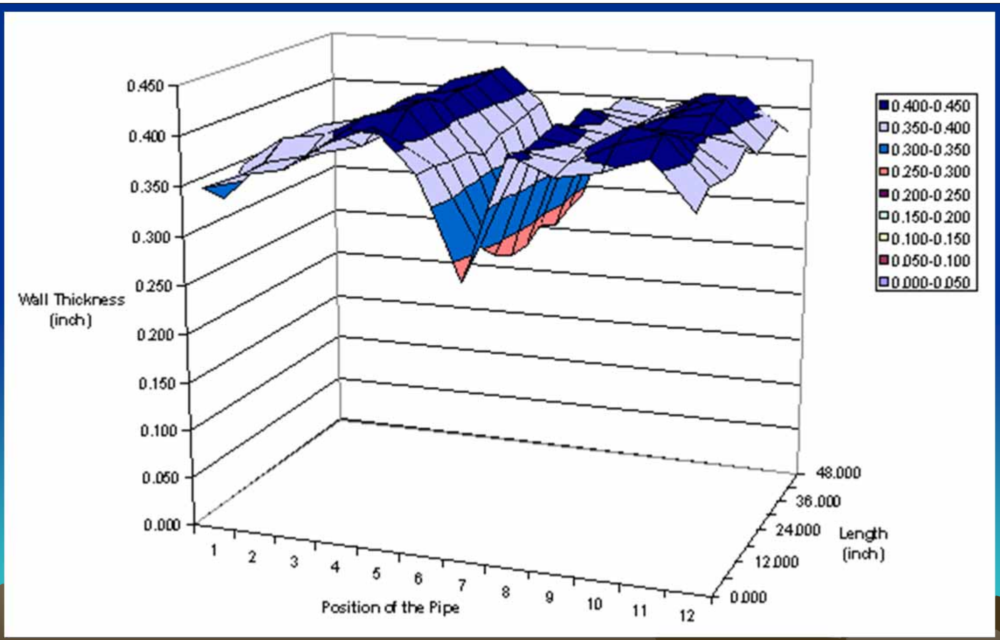


# Conclusions

- A fiber optic distributed strain and temperature sensor (DSTS) has been used to identify several inner wall cutouts in an end-capped steel pipe successfully.
- Larger strains are observed in the big defective region.
- Between the small defective regions, the 60% depleted wall experienced larger strains than the 50% depleted wall.
- DSTS has been used to identify wall thickness change of steel pipe caused by oil sand erosion successfully.

# Acknowledgement


Dr. Gordon P. Gu

Mr. A. Doiron

Dr. S. Papavinasam

CANMET Materials Technology Laboratory

Ottawa, Ontario, Canada

Thanks for your attention.

Questions?